Unimolecular Reaction Kinetics of $CF_2ClCF_2CH_3$ and $CF_2ClCF_2CD_3$: Experimental Evidence for a Novel 1,2-FCl Rearrangement Pathway†

Maria O. Burgin, George L. Heard, Jaime M. Martell, and Bert E. Holmes*

Department of Chemistry, The University of North Carolina at Asheville, One University Heights, Asheville, North Carolina 28804-8511

Received: July 13, 2000; In Final Form: November 16, 2000

Chemically activated $CF_2ClCF_2CH_3$ and $CF_2ClCF_2CD_3$, containing 98.5 and 100 kcal/mol of internal energy, respectively, were formed in the gas phase from the combination of CF_2ClCF_2 and CH_3 or CD_3 radicals, respectively. These radicals were generated from the UV photolysis of CF_2ClCF_2I and CH_3I or CD_3I. The decomposition products were $CF_2ClCF{=}CH_2$ ($CF_2ClCF{=}CD_2$) from a 2,3-HF (DF) elimination and $CF_3CF{=}CH_2$ ($CF_3CF{=}CD_2$) suggesting a 1,3-HCl (DCl) elimination reaction. The 1,3-HCl elimination mechanism appears to be a two-step process; a 1,2-FCl rearrangement, producing $CF_3ClCFClCH_3$ ($CF_3CFClCD_3$), followed by a 2,3-HCl (DCl) elimination. Unimolecular rate constants for $CF_2ClCF_2CH_3$ ($CF_2ClCF_2CD_3$) were $5.3 \pm 2.1 \times 10^5$ s^{-1} ($1.8 \pm 0.7 \times 10^5$ s^{-1}) for 2,3-HF (DF) loss and $3.6 \pm 1.4 \times 10^4$ s^{-1} ($2.3 \pm 0.9 \times 10^4$ s^{-1}) for the 1,2-FCl rearrangement. The branching ratio was 13.5 ± 3 (7.8 ± 1.6) favoring the HF (DF) process. The isotope effect for 2,3-HF/DF was 2.9 ± 0.6, while for the FCl rearrangement, it was considerably smaller at 1.5 ± 0.3. The $CF_3CFClCH_3$ and the $CF_3CFClCD_3$, formed by the 1,2-FCl migration, react by loss of HCl (DCl) with rate constants of $2.1 \pm 1.3 \times 10^7$ s^{-1} ($7.9 \pm 4.8 \times 10^6$ s^{-1}) and an isotope effect of 2.7 ± 0.8. Theoretical rate constants, branching ratio and isotope effects were calculated using RRKM theory and density functional theory to compute all of the data necessary for the RRKM calculations. The agreement between the experimental and computed kinetic data suggests that the 1,3-HCl elimination is a two-step mechanism consisting of a 1,2-FCl rearrangement followed by a 2,3-HCl elimination.

1. Introduction

Unimolecular reaction paths for energized haloalkanes include elimination of HX (X = F, Cl, Br and I) and rupture of C−X, C−C and C−H bonds.[1,2] Fission of the C−C, C−F or C−H bonds will not normally occur because their bond dissociation energies are much greater than the threshold energy, E_o, for HX elimination. Carbon−halogen bond rupture is generally only important for iodides and bromides when the C−X bond dissociation energy is comparable to the E_o for HX elimination.[1] However, a recent investigation of shock heated alkyl iodides[3] did find that 1,2-HI elimination can be the dominant channel; the branching fraction (C−I bond rupture versus 1,2-HI elimination) was 0.6−0.9 for primary iodides, 0.2−0.4 for secondary iodides and less than 0.05 for tertiary iodides.

The most common elimination mechanism is the 1,2-HX channel but 1,1-elimination is also known.[4−7] When 1,1- and 1,2-pathways are both open for an alkyl fluoride or chloride the 1,1-elimination rate constant is typically one-tenth of the rate constant for the 1,2-channel.[4] However, the 1,1-HCl unimolecular rate constant may be slightly larger than the rate constant for the 1,2-HF pathway in CF_3CH_2Cl.[6] There are few reports,[8−11] of 1,3-HX elimination and all involve 1,3-HCl loss from neopentyl halides or norbornyl halides; these elimination/rearrangements are known as Wagner−Meerwein rearrangements. Most of these Wagner−Meerwein rearrangements were with 2,2-dimethyl-1-chloropropane or 2,2-dimethyl-1-bromopropane that lack a hydrogen on the carbon adjacent to the halogen so the 1,2-HX channel was not open and a 2,1-methyl shift accompanied the elimination process. Deuterium labeling experiments showed that both 1,1- and 1,3-HX eliminations occur for the 2,2-dimethyl-1-chloropropane and if the product yields are corrected for the number of available hydrogens and for the isotope effect then the threshold energies appear to be similar for the two mechanisms.[11] In summary, for haloalkanes the E_o(1,2-HX) increases along the series HI, HBr, HCl to HF; for a specific halogen the E_o(1,2-HX) is smaller than for E_o(1,1-HX); and the E_o(1,1-HX) may be comparable to the E_o(1,3-HX). Little is known about the isotope effect for either the 1,1- or the 1,3-HX mechanism, while the isotope effect for 1,2-HX loss has been extensively investigated.[12,13]

In contrast to haloalkanes, the 1,1-HX elimination may dominant the 1,2-HX process in haloalkenes following excitation by absorption of UV radiation or multiple IR photons. In some cases the electronically excited reactant internally converts to the ground electronic state prior to dissociation[14,15] but in others[16,17] the decomposition occurs on excited electronic surfaces. Haloalkanes have also been energized by UV and IRMP absorption. Using 193 nm light no HCl elimination was observed[18] for excited CH_3CF_2Cl and CH_3CFCl_2 in contrast to the HF and HCl loss found[12] for vibrationally excited, ground electronic state molecules, suggesting the reaction occurred on upper electronic energy surfaces following UV excitation. Photoexcitation has been of great use in understanding the reactions of these molecules but care must be exercised to determine whether the decomposition occurs on the ground or excited-state electronic energy surface.

A motivation for this work is to prepare a chemically activated molecule that might exhibit both 1,3-and 1,2-HX elimination

† Part of the special issue "Harold Johnston Festschrift".

10.1021/jp002511d CCC: $20.00
Published on Web 01/06/2001

and to determine the isotope effect for the 1,3-elimination process. Since the E_o(1,2-HCl) is lower than the E_o(1,2-HF) it was hoped that 1,3-HCl might be competitive with 1,2-HF loss if the 1,2-HCl was not open. Our proposed study will focus on the unimolecular pathways, occurring on the ground-state potential energy surface, for $CF_2ClCF_2CH_3$ and $CF_2ClCF_2CD_3$. Chemically activated $CF_2ClCF_2CH_3$ ($CF_2ClCF_2CD_3$) will be prepared by the combination of CF_2ClCF_2 and CH_3 (CD_3) radicals. The radicals will be generated by photolysis of the appropriate iodide, illustrated in reaction 1a, and the radical combination process that produced the chemically activated halopropanes are shown in reaction 1b.

$$CF_2ClCF_2I + CD_3I\ (CH_3I) \xrightarrow{Hg_2I_2,\ h\nu} CF_2ClCF_2 + CD_3\ (CH_3) + 2HgI_2(s) \quad (1a)$$

$$CF_2ClCF_2 + CD_3\ (CH_3) \rightarrow CF_2ClCF_2CD_3{*}\ (CF_2ClCF_2CH_3{*}) \quad (1b)$$

Reaction 1b prepares the 1-chloro-1,1,2,2-tetrafluoropropane with about 100 kcal/mol of energy in vibrational and rotational motion and the * denotes that the molecule is chemically activated. The alkene products that were observed are consistent with the following unimolecular pathways for $CF_2ClCF_2CH_3$*. A similar set of reactions for $CF_2ClCF_2CD_3$* will be shown in the Results and Discussion section. Reaction 3 is collisional deactivation that removes internal energy so the molecule cannot react because it contains less energy than the E_o of the elimination reactions.

$$CF_2ClCF_2CH_3{*} \xrightarrow{k_{2,3-HF}} CF_2ClCF{=}CH_2 + HF \quad (2a)$$

$$\xrightarrow{k_{1,3-HCl}} CF_3CF{=}CH_2 + HCl \quad (2b)$$

$$\xrightarrow{k_M[M]} CF_2ClCF_2CH_3 \quad (3)$$

Reaction 2b suggests that the 1,3-HCl elimination is accompanied by a 2,1-F migration giving the $CF_3CF{=}CH_2$, however we cannot rule out the possibility that tetrafluorocyclopropane might also form.

2. Experimental Section

Pyrex vessels of volumes ranging from 14.85 to 3505.6 cm^3 containing between 1.05 and 5.22 μmols of methyl iodide or deuterated methyl iodide, between 0.629 and 0.0808 μmols of 1-chloro-2-iodo-1,1,2,2-tetrafluoroethane, and small amounts of mercury and mercury(I) iodide were photolyzed with a high-pressure 200 W mercury lamp. The presence of mercury(I) iodide in the vessels during photolysis aids[19] in formation of the methyl and 2-chloro-1,1,2,2-tetrafluoroethyl radicals. Photolysis times were between 2 and 30 min, at room-temperature resulting in the conversion of about 10% of the reactants to products. All gases were manipulated on grease-free vacuum lines and an MKS 270C High Accuracy Signal Conditioner was used to measure pressures of the reactants during sample preparation.

Product identification was based on the mass spectral fragmentation pattern from a Shimadzu QP5000 GC/MS equipped with a 105 m Rtx-200 column. The following products were observed: $CF_3CF{=}CH_2$ (resulting from the 1,3-HCl elimination), $CF_2ClCF{=}CH_2$ (resulting from a 2,3-HF elimination), and $CF_2ClCF_2CH_3$. A commercial sample of $CF_3CF{=}CH_2$ was available to confirm identity of the alkene formed by 1,3-HCl elimination. We searched for, but found no evidence for 1,1,2,2-tetrafluorocyclopropane, which might form by a 1,3-HCl elimination followed by ring closure of the $CF_2CF_2CH_2$ biradical. We also searched for the product from the 1,2-FCl rearrangement of $CF_2ClCF_2CH_3$ but found no evidence for $CF_3CFClCH_3$, even though an authentic sample was available for verification.

TABLE 1: Mass Spectral Fragmentation Data at 70 EV (*m/e*, Relative Abundance, and Assignment)

$CF_3CF{=}CH_2$			$CF_3CF{=}CD_2$		
m/e	RA	assignment	*m/e*	RA	assignment
69	100	CF_3^+	69	100	CF_3^+
64	99	$C_2F_2H_2^+$	66	79	$C_2F_2D_2^+$
114	77	$C_3F_4H_2^+$	116	50	$C_3F_4D_2^+$
95	33	$C_3F_3H_2^+$	47	46	$C_2FD_2^+$
113	26	$C_3F_4H^+$	97	41	$C_3F_4D_2^+$
75	10	$C_3F_2H^+$	114	15	$C_3F_3D^+$

$CF_2ClCF{=}CH_2$			$CF_2ClCF{=}CD_2$		
m/e	RA	assignment	*m/e*	RA	assignment
95	100	$C_3F_3H_2^+$	97	100	$C_3F_3D_2^+$
69	47	CF_3^+	69	63	CF_3^+
130	19	$C_3F_3{}^{35}ClH_2^+$	31	23	CF^+
75	10	$C_3F_2H^+$	47	18	$C_2D_2F^+$
132	6	$C_3F_3{}^{37}ClH_2^+$	132	14	$C_3F_3{}^{35}ClD_2^+$

$CF_2ClCF_2CH_3$			$CF_2ClCF_2CD_3$		
m/e	RA	assignment	*m/e*	RA	assignment
65	100	$C_2F_2H_3^+$	68	100	$C_2F_2D_3^+$
115	58	$C_3F_4H_3^+$	118	27	$C_3F_4D_3^+$
45	30	$C_2FH_2^+$	47	18	$C_2FD_2^+$
51	20	CF_2H^+	52	11	CF_2D^+
85	16	$CF_2{}^{35}Cl^+$	31	9	CF^+

$CF_2ClCF_2CF_2CF_2Cl$		
m/e	RA	assignment
85	100	$CF_2{}^{35}Cl^+$
69	52	CF_3^+
87	32	$CF_2{}^{37}Cl^+$
147	21	$C_3F_4{}^{35}Cl^+$
119	15	$C_2F_5^+$

Kinetic analyses of the reaction mixtures were conducted on the Shimadzu GC-14A with flame ionization detector and a Shimadzu CR501 Chromatopac Integrator acquired and integrated peak area. A Rtx-200 column of length 105 m and diameter of 0.53 millimeters was used with the following temperature program: an initial temperature of 35 °C for a period of 20 min, at which point the temperature increased at a rate of 12°/min until the oven reached a final temperature of 190 °C. Using these conditions the retention times of the primary compounds of interest were as follows: C_2H_6 at 9.5 min; $CF_3CF{=}CH_2$ at 10.1 min; $CF_2ClCF{=}CH_2$ at 12.7 min; $CF_2ClCF_2CH_3$ at 13.4 min; $CF_2ClCF_2CF_2CF_2Cl$ at 16.1 min; CH_3I at 16.5 min; and CF_2ClCF_2I at 28.0 min. The C_2H_6 and $CF_2ClCF_2CF_2CF_2Cl$ were formed by the combination of methyl and 2-chloro-1,1,2,2-tetrafluoroethyl radicals, respectively. Table 1 contains mass spectra for these products and the deuterated anologues.

Direct calibration of the flame-ionization detector was impossible since authentic samples were not available for $CF_2ClCF{=}CH_2$ and $CF_2ClCF_2CH_3$. We have found[20] that response factors for halogenated propenes/propanes are near one and values of 1.0 were adopted for this study.

3. Results and Discussion

3.1. Experimental Results. The results that will be presented in this section will suggest that the 1,3-HCl elimination process

is actually a two-step mechanism; the first step is a 1,2-FCl interchange followed by a 2,3-HCl elimination. The unimolecular reactions for $CF_2ClCF_2CD_3$* are

$$CF_2ClCF_2CD_3^* \xrightarrow{k_{1,2-FCl}} CF_3CFClCD_3^* \quad (4a)$$

$$\xrightarrow{k_{2,3-DF}} CF_2ClCF{=}CD_2 + DF \quad (4b)$$

$$\xrightarrow{k_M[M]} CF_2ClCF_2CD_3 \quad (5)$$

The chemically activated $CF_3CFClCD_3$* formed by reaction 4a contains all of the initial energy that the $CF_2ClCF_2CD_3$* contained plus some extra energy because the computational results, presented below, suggest that the 1,2-FCl rearrangement process is exothermic by 3.3 kcal/mol. The unimolecular reactions of the chemically activated $CF_3CFClCD_3$* are

$$CF_3CFClCD_3^* \xrightarrow{k_{2,3-DCl}} CF_3CF{=}CD_2 + DCl \quad (6a)$$

$$\xrightarrow{k_{2,3-DF}} CF_3CCl{=}CD_2 + DF \quad (6b)$$

$$\xrightarrow{k_M[M]} CF_3CFClCD_3 \quad (7)$$

The computational results predict that the E_o(2,3-DCl) for $CF_3CFClCD_3$* is 10 kcal/mol lower in energy than the E_o(1,2-FCl) for the $CF_2ClCF_2CD_3$* (see Figure 6); so once the $CF_2ClCF_2CD_3$* rearranges to $CF_3CFClCD_3$*, it is reasonable to assume that all of the $CF_3CFClCD_3$* will eliminate DCl unless it is stabilized by collisions, reaction 7. If all of the $CF_3CFClCD_3$* reacts by reaction 6a then the $CF_3CF{=}CD_2$ will equal the $CF_3CFClCD_3$* yield and the following two equations can be written.

$$[CF_3CF{=}CD_2]/[CF_2ClCF_2CD_3] = k_{1,2-FCl}/k_M[M] \quad (8)$$

$$[CF_2ClCF{=}CD_2]/[CF_3CF{=}CD_2] = k_{2,3-DF}/k_{1,2-FCl} \quad (9)$$

It is reasonable to assume that $CF_3CFClCD_3$* eliminates DCl rather than DF because the DCl/DF branching ratio for similar chlorofluoroalkanes is very large: 25 for CF_2ClCD_3 and 80 for $CFCl_2CD_3$.[12,21]

Since the product ratio equals the rate constant ratio then analysis of reactions 4b and 5 leads to

$$[CF_2ClCF{=}CD_2]/[CF_2ClCF_2CD_3] = k_{2,3-DF}/k_M[M] \quad (10)$$

The products from the decomposition reactions, reactions 4a, 4b, 6a and 6b are designated as D and products from the collisional stabilization, reactions 5 and 7, are designated S. Equations 8 and 10 should be linear when D/S is plotted vs $1/P$, where $[M] = P$. It seems reasonable to use the strong collision assumption since the bath gas mixture is methyl iodide and 1-chloro-2-iodo-1,1,2,2-tetrafluoroethane and since only higher pressure data where D/S < 1.5 will be plotted.

Data are plotted using eqs 8 and 10 in Figure 1 for $CF_2ClCF_2CH_3$ and in Figure 2 for $CF_2ClCF_2CD_3$. As expected for a well-behaved unimolecular reaction system the intercepts are nearly zero and the data is linear when D/S < 1.5. The slopes are k_i/k_M and the unimolecular rate constants, k_i, are determined by using collision theory to calculate $k_M = 1.11 \times 10^7$ (s Torr)$^{-1}$. The kinetic isotope effect is the ratio of the slopes of the data in Figures 1 and 2. For example, the squares represent HF or DF elimination so the $k_{HF}/k_{DF} = 2.9$. The kinetic isotope effect for the 1,2-FCl rearrangement is $k_H/k_D = 1.5$. It should be noted that an isotope effect this small, first suggested to us

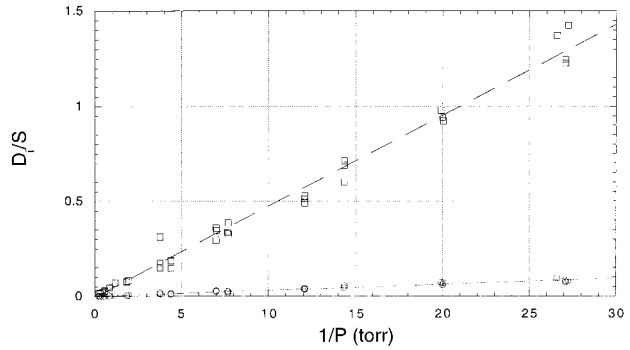

Figure 1. D_i/S versus reciprocal pressure plot for the 2,3-HF elimination (squares) and the 1,2-FCl rearrangement of $CF_2ClCF_2CH_3$ (circles). The slope is 0.0479 Torr, the intercept is −0.00582 and the correlation coefficient is 0.994 for HF loss. For the FCl rearrangement the slope is 0.00321 Torr, the intercept is 0.000287 and the correlation coefficient is 0.987

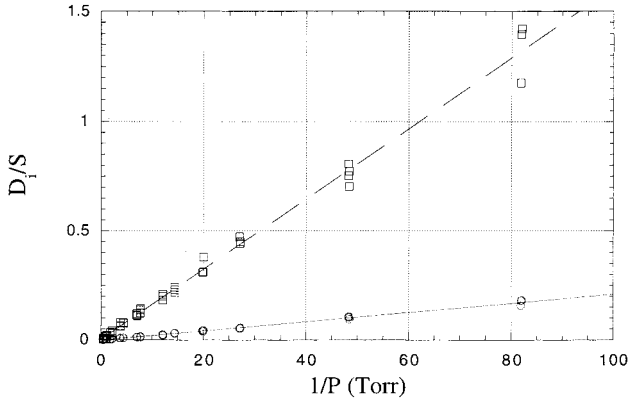

Figure 2. D_i/S versus reciprocal pressure plot for the 2,3-DF elimination (squares) and the 1,2-FCl rearrangement of $CF_2ClCF_2CD_3$ (circles). The slope is 0.0161 Torr, the intercept is 0.00297 and the correlation coefficient is 0.996 for HF loss. For the FCl rearrangement the slope is 0.00211 Torr, the intercept is 0.000981 and the correlation coefficient is 0.997.

that the HCl elimination was not a direct process. Table 4 summarizes the rate constants and kinetic isotope data.

The branching ratio $k_{2,3-HF}/k_{1,2-FCl}$ is the ratio of the slopes in Figure 1 for $CF_2ClCF_2CH_3$ ($k_{2,3-HF}/k_{1,2-FCl} = 14.7$) and $k_{2,3-DF}/k_{1,2-FCl}$ is the ratio of the slopes in Figure 2, ($k_{2,3-DF}/k_{1,2-FCl} = 7.83$). The branching ratio can also be determined using eq 9. Figures 3 and 4, which include data at lower pressures, are plots of eq 9 for $CF_2ClCF_2CH_3$ and $CF_2ClCF_2CD_3$, respectively and these data give $k_{2,3-HF}/k_{1,2-FCl} = 13.5$ and $k_{2,3-DF}/k_{1,2-FCl} = 7.8$ when $1/P > 50$. The branching ratios determined from Figures 3 and 4 are probably more reliable than the ratio of slopes from Figures 1 and 2 because at low pressures all of the chemically activated reactant decomposes so that the yield of decomposition products are the greatest. We adopt these limiting low-pressure values for the branching ratio. Note that in Figure 4 the natural log of $1/P$ is plotted to spread out the data for better illustration of the variation of the branching ratio with pressure in the high-pressure region; i.e., smaller $1/P$.

Data in Figures 3 and 4 would be independent of pressure and horizontal if both of the alkene products were formed from the same reactant. The upward curvature evident in Figures 3 and 4 is probably caused by the onset of reaction 7 at higher pressures, i.e., some of the $CF_3CFClCH_3$* or $CF_3CFClCD_3$* is collisionally stabilized as the pressure is increased. Collisional deactivation of the activated molecule reduces the yield of $CF_3CF{=}CH_2$ or $CF_3CF{=}CD_2$ relative to $CF_2ClCF{=}CH_2$ or CF_2-

TABLE 2: Summary of Experimental Rate Constants and RRKM Models[a] for 1-Chloro-1,1,2,2-tetrafluoropropane-d_0 and -d_3.

	molecules		activated complexes, elimination or transfer of			
	$CClF_2CF_2CH_3$	$CClF_2CF_2CD_3$	2,3-HF	2,3-DF	1,2-FCl-d_0	1,2-FCl-d_3
vibrational frequencies, cm^{-1} (degeneracies)[a]	3133 (3)	2299 (3)	3210 (2)	2363 (2)	3136 (3)	2300 (3)
	1294 (8)	1143 (8)	1443 (8)	1306 (4)	1455 (9)	1474 (3)
	949 (3)	845 (3)	1024 (5)	1007 (4)	1065 (6)	1077 (4)
	619 (3)	593 (3)	683 (3)	692 (5)	764 (1)	801 (3)
	375 (6)	364 (6)	422 (6)	390 (6)	551 (3)	494 (4)
	206 (3)	180 (3)	222 (4)	218 (4)	311 (7)	286 (6)
	71 (1)[b]	68 (1)	75 (1)	74 (1)	166 (3)	148 (3)
moments of inertia, I (amu-A^2)	795, 1212, 1336	843, 1259, 1386	860, 1205, 1396	900, 1257, 1439	904, 1119, 1351	970, 1148, 1401
moments of inertia $(I^{\ddagger}/I)^{1/2}$			1.06	1.05	1.03	1.03
reaction path degeneracy			4	4	0.67	0.67
preexponential factor,[c] s^{-1}			1.88×10^{13}	1.70×10^{13}	1.89×10^{13}	1.86×10^{13}
activation entropy (cal/K)			3.15	2.97	−0.06	−0.10
E_o, kcal/mol			63.8	64.8	62.5	62.5
$\langle E \rangle$, kcal/mol			98.5	100	98.5	100
k_a(exptl), s^{-1}			5.3×10^5	1.8×10^5	3.6×10^4	2.3×10^4
k_a(calcd), s^{-1}			2.32×10^6	9.69×10^5	5.80×10^5	4.19×10^5
$[k_a^H/k_a^D]$(exptl)			2.9 ± 0.6			1.5 ± 0.3
$[k_a^H/k_a^D]$(calcd)			2.39			1.38
$[k_a^{HF(DF)}/k_a^{FCl}]$(exptl)	13.5 ± 3	7.8 ± 1.6				
$[k_a^{HF(DF)}/k_a^{FCl}]$(calcd)	4.00	2.31				

[a] Moments of inertia and vibrational frequencies from DFT using B3PW91/6-311++G(2d,p). [b] Hindered rotor treated as a torsion. [c] Partition function form for unit reaction path degeneracy at 800 K.

TABLE 3: Summary of Experimental Rate Constants and RRKM Models[a] for 2-Chloro-1,1,1,2-tetrafluoropropane-d_0 and -d_3.

	molecules		activated complexes for 2,3- elimination			
	$CF_3CFClCH_3$	$CF_3CFClCD_3$	2,3-HF	2,3-DF	2,3-HCl	2,3-DCl
vibrational frequencies, cm^{-1} (degeneracies)[a]	3128 (3)	2294 (3)	3198 (2)	2354 (2)	3184 (2)	2343 (2)
	1272 (9)	1144 (8)	1386 (6)	1262 (5)	1476 (4)	1340 (4)
	830 (3)	803 (4)	1006 (4)	992 (3)	1130 (6)	990 (5)
	567 (3)	551 (3)	680 (3)	687 (5)	640 (5)	641 (6)
	355 (5)	342 (5)	476 (5)	439 (5)	388 (4)	347 (4)
	213 (3)	187 (3)	231 (5)	224 (5)	205 (3)	200 (3)
	72 (1)[b]	70 (1)	79 (1)	78 (1)	83 (2)	83 (2)
moments of inertia, I (amu-A^2)	799, 1199, 1329	857, 1231, 1377	866, 1201, 1399	918, 1239, 1438	818, 1434, 1600	869, 1471, 1639
moments of inertia $(I^{\ddagger}/I)^{1/2}$			1.07	1.06	1.21	1.20
reaction path degeneracy			2	2	2	2
thermal preexponential factor,[c] s^{-1}			1.95×10^{13}	1.82×10^{13}	4.97×10^{13}	4.56×10^{13}
activation entropy (cal/K)			1.84	1.72	3.76	3.51
E_o, kcal/mol			60.9	61.8	55.4	56.5
$\langle E \rangle$, kcal/mol			101.8	103.3	101.8	103.3
k_a(exptl), s^{-1}			not detected	not detected	2.1×10^7	7.9×10^6
k_a(calcd), s^{-1}			8.2×10^6	3.9×10^6	1.6×10^8	7.8×10^7
$[k_a^H/k_a^D]$(exptl)			not detected			2.7 ± 0.8
$[k_a^H/k_a^D]$(calcd)			2.1			2.1
$[k_a^{HCl(DCl)}/k_a^{HF(DF)}]$(exptl)	not detected	not detected				
$[k_a^{HCl(DCl)}/k_a^{HF(DF)}]$(calcd)	20.	20.				

[a] Moments of inertia and vibrational frequencies from DFT using B3PW91/6-311++G(2d,p). [b] Hindered rotor treated as a torsion. [c] Partition function form for unit reaction path degeneracy at 800 K.

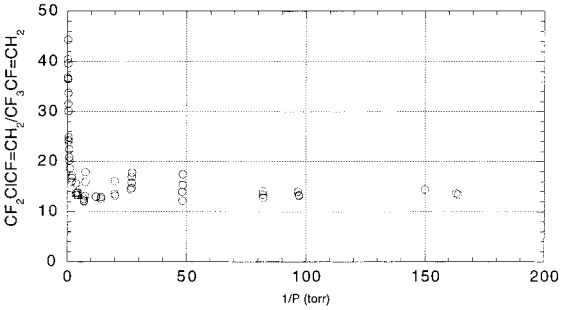

Figure 3. Experimental yield of $[CF_2ClCF{=}CH_2]/[CF_3CF{=}CH_2]$ versus reciprocal pressure for the $CF_2ClCF_2CH_3$ system. At lower pressures the branching ratio is constant at 13.5.

$ClCF{=}CD_2$, respectively. In other words, at the highest pressures only a very small fraction of the energized $CF_2ClCF_2CH_3$ has energy in the proper motion to cause the 1,2-FCl rearrangement leading to $CF_3CFClCH_3$. The onset of the upward curvature in Figure 3 is for $1/P < 1.0$ and this corresponds to a D/S, for the 1,2-FCl migration, in Figure 1 of 0.0025. Only at these high pressures, i.e., high collision frequency, will there be a chance for a deactivating collision of $CF_3CFClCH_3$ to occur, before the energy in the 1,2-FCl rearrangement motion migrates to the proper mode to cause the 2,3-HCl elimination leading to CF_3-$CF{=}CH_2$.

The yield of collisionally stabilized $CF_3CFClCH_3$ can be extracted from the data in Figure 3. The $k_{2,3-HF}/k_{1,2-FCl} = [CF_2$-$ClCF{=}CH_2]/[CF_3CFClCH_3{*}]$ and this must equal 13.5, the low-pressure limit given in Figure 3. Mass balance gives $[CF_3CF$-$ClCH_3{*}] = [CF_3CF{=}CH_2] + [CF_3CCl{=}CH_2] + [CF_3CFClCH_3]$. As just mentioned above the elimination of HF from CF_3-$CFClCH_3{*}$ must be a factor of 25−80 smaller than the elimination of HCl, so it is reasonable to assume that reaction 6b can be neglected. Thus, the $[CF_3CFClCH_3{*}]$ approximately

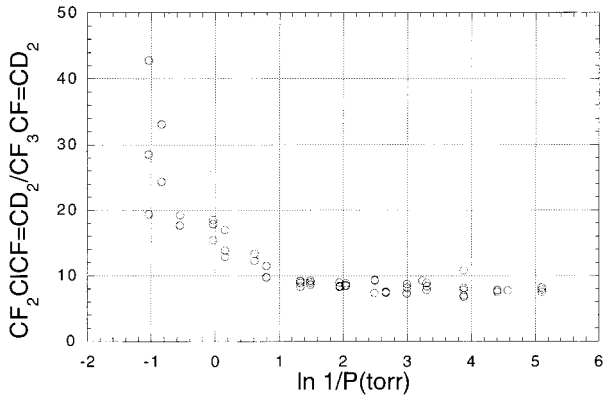

Figure 4. Experimental yield of $[CF_2ClCF{=}CD_2]/[CF_3CF{=}CD_2]$ versus the ln of the reciprocal pressure for the $CF_2ClCF_2CD_3$ system. At lower pressures the branching ratio is constant at 7.6. The data are plotted versus the ln 1/*P* to spread out the data and better illustrate the upward curvature of the branching ratio at higher pressures.

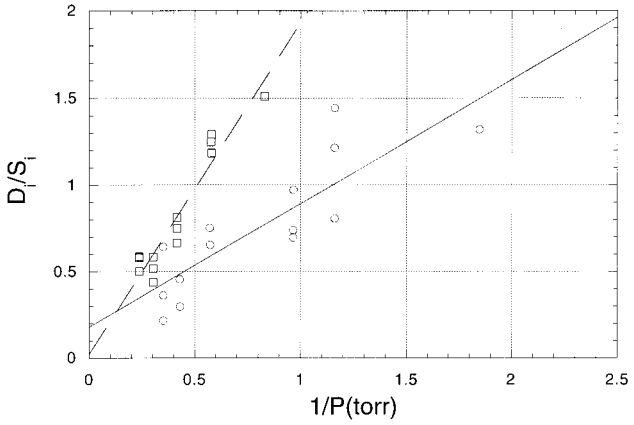

Figure 5. D_i/S versus reciprocal pressure plot for the 2,3-HF elimination (squares) from $CF_2ClCF_2CH_3$ and the 2,3-DF elimination from $CF_2ClCF_2CD_3$ (circles). The slope is 1.91 Torr, the intercept is 0.0216 and the correlation coefficient is 0.954 for HF loss. For the DF loss the slope is 0.714 Torr, the intercept is 0.179 and the correlation coefficient is 0.844.

equals the sum of the $[CF_3CF{=}CH_2]$ and $[CF_3CFClCH_3]$ yields. The branching ratio then becomes

$$k_{2,3-HF}/k_{1,2-FCl} = 13.5 = [CF_2ClCF{=}CH_2]/([CF_3CF{=}CH_2] + [CF_3CFClCH_3]) \quad (11)$$

Since the $[CF_2ClCF{=}CH_2]$ and $[CF_3CF{=}CH_2]$ are measured the $[CF_3CFClCH_3]$ can then be calculated using eq 11. These data then give

$$[CF_3CF{=}CH_2]/[CF_3CFClCH_3] = k_{2,3-HCl}/k_M[M] \quad (12)$$

and the $k_{2,3-HCl}$ can be determined from the usual D/S vs 1/*P* plot using eq 12; see Figure 5. It is gratifying to see that the data are linear with an intercept near zero and the $k_{2,3-HCl} = 2.1 \times 10^7\ s^{-1}$, using the same k_M as for the $CF_2ClCF_2CH_3$* system. A similar analysis for $CF_3CFClCD_3$* gave the results in Figure 5 and, although the data are more scattered, the $k_{2,3-DCl} = 7.9 \times 10^6\ s^{-1}$. This kinetic isotope effect is 2.7. Finally, we note that the onset of the upward curvature in Figures 3 and 4 occurs when the 1/*P* is less than 1.0. This pressure corresponds to a D/S, for 1,2-FCl rearrangement, less than 0.0025 in Figure 1 and less than 0.0016 in Figure 2. This illustrates that the yield of $CF_3CFClCH_3$ would be at least 400 times lower than the $CF_2ClCF_2CH_3$ yield. We attempted to verify the presence of

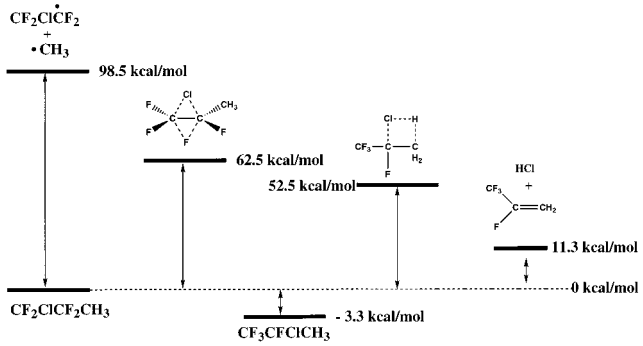

Figure 6. Energy versus the reaction coordinate profile for the two-step mechanism converting $CF_2ClCF_2CH_3$ into $CF_3CF{=}CH_2$ + HCl. DFT methods were used to compute the energies

$CF_3CFClCH_3$ but were not able to separate it from the $CF_2ClCF_2CH_3$. Because these two chlorofluoropropanes could not be resolved and because the yield of $CF_2ClCF_2CH_3$ was at least 400 times greater than the $CF_3CFClCH_3$ yield, our inability to observe $CF_3CFClCH_3$ is not surprising.

These unimolecular rate constants and kinetic isotope effect for $CF_2ClCF_2CH_3$ and $CF_3CFClCD_3$ can be compared to unimolecular dehydrohalogenations for similar haloalkanes. The $k_{2,3-HF} = 5.3 \times 10^5\ s^{-1}$ for 2,3-HF loss from $CF_2ClCF_2CH_3$, activated by the combination of CF_2ClCF_2 and CH_3 radicals, and is gratifyingly similar to the $k_{2,3-HF} = 4.5 \times 10^5\ s^{-1}$ for 2,3-HF from $CF_3CF_2CH_3$ activated by combination of CF_3CF_2 and CH_3 radicals.[20] Kinetic isotope effects for chemically activated haloalkanes range from 2.3 to 4.4 for the HF elimination reaction; for example, k_{HF}/k_{DF}'s are 2.3 (CH_2FCH_3/CH_2FCD_3),[22] 2.7 (CHF_2CH_3/CHF_2CD_3),[23] 3.0 ($CClF_2CH_3/CClF_2CD_3$),[21] and 4.4 for (CCl_2FCH_3/CCl_2FCD_3).[12] For $CF_2ClCF_2CH_3/CF_2ClCF_2CD_3$ we find $k_{HF}/k_{DF} = 2.9 \pm 0.6$, which is consistent with these other nonequilibrium kinetic isotope effects. A similar range has been found for k_{HCl}/k_{DCl} with 1,2-HCl elimination, i.e., 2.1 for (CH_2ClCH_3/CH_2ClCD_3),[13a] 3.2 for ($CClF_2CH_3/CClF_2CD_3$),[21] and 4.4 for (CCl_2FCH_3/CCl_2FCD_3).[12] For $CF_3CFClCH_3/CF_3CFClCD_3$ we find $k_{HCl}/k_{DCl} = 2.7 \pm 0.8$. The kinetic isotope effect for the reaction that is formally a 1,3-HCl/DCl elimination was 1.5 ± 0.3. We believe that this is actually the isotope effect for the 1,2-FCl rearrangement and such a small isotope effect suggested that the mechanism was not a direct 1,3-HCl elimination. Figure 6 shows the computed potential energy profile for the 1,3-HCl process, computational details are in the next section. The threshold energy barrier for the 1,2-FCl rearrangement is 10 kcal/mol higher the E_o for the 2,3-HCl process, and since the rate-limiting step does not involve C−H motion the H/D kinetic isotope effect is small.

3.2. Computational Results. Several mechanisms can be suggested for the production of the $CF_3CF{=}CH_2$ product. For example, a 1,3-HCl elimination has been proposed for chloroalkanes when the 1,2-HCl channel is not available.[11] A similar pathway for $CF_2ClCF_2CH_3$ could be a concerted 1,3-HCl elimination occurring concurrently with a 2,1-F migration. Alternatively, a biradical intermediate could be formed by the 1,3-HCl elimination with subsequent migration of the atomic fluorine. We attempted to use density functional theory, DFT, *ab initio* methods to locate a 1,3-HCl transition state with a threshold energy, E_o, near the E_o's for 1,2-dehydrohalogenation, but were not successful. Computational details are in the following paper in this issue.[24] We did find a 1,2-FCl rearrangement converting $CF_2ClCF_2CH_3$ to $CF_3CFClCH_3$ with a threshold energy near 60 kcal/mol, depending upon the DFT method and the basis set. If this process were followed by 2,3-

TABLE 4: Summary of Experimental and Computed Kinetic Results (s^{-1})for $CF_2ClCF_2CH_3/CF_2ClCF_2CD_3$ and for $CF_3CFClCH_3/CF_3CFClCD_3$

A. $CF_2ClCF_2CH_3$ and $CF_2ClCF_2CD_3$

	$k_{HF(DF)}$	k_{FCl}	k_{HF}/k_{FCl}
	1. $CF_2ClCF_2CH_3$		
explt	$(5.3 \pm 2.1) \times 10^5$	$(3.6 \pm 1.4) \times 10^4$	13.5 ± 3
calcd	2.32×10^6	5.80×10^5	4.00
	2. $CF_2ClCF_2CD_3$		
explt	$(1.8 \pm 0.7) \times 10^5$	$(2.3 \pm 0.9) \times 10^4$	7.8 ± 1.6
calcd	9.69×10^5	4.19×10^5	2.31
k_H/k_D			
exptl	2.9 ± 0.6	1.5 ± 0.3	
calcd	2.39	1.38	

B. $CF_3CFClCH_3$ and $CF_3CFClCD_3$

	$k_{HCl(DCl)}$	$k_{HF(DF)}$
	1. $CF_3CFClCH_3$	
explt	$(2.1 \pm 1.3) \times 10^7$	not detected
calcd	1.6×10^8	8.2×10^6
	2. $CF_3CFClCD_3$	
explt	$(7.9 \pm 4.8) \times 10^6$	not detected
calcd	7.8×10^7	3.9×10^6
k_H/k_D		
exptl	2.7 ± 0.8	not detected
calcd	2.1	2.1

HCl elimination from the $CF_3CFClCH_3$ then the product would be the $CF_3CF{=}CH_2$. These 1,2-FCl migrations were computationally investigated for several molecules of the type $CF_2ClCFXCY_3$ (X = H, F and Y = H, D, F) and the threshold barriers were between 55 and 70 kcal/mol and the rearranged $CF_3CClXCY_3$ was as much as 10 kcal/mol more stable than the reactant. The 1,2-FCl rearrangement transition state geometry is planar with Cl and F in an anti-geometry and each migrating atom was a nearly symmetric 3-centered, bridged structure. Figure 6 is a potential energy profile for this mechanism. More details about the calculations and about the 1,2-FCl rearrangement transition state are in the following paper in this issue.

To provide evidence that this elimination reaction, formally a 1,3-HCl elimination, actually is a stepwise process involving a 1,2-FCl rearrangement followed by a 2,3-HCl elimination, we calculated threshold energies for both processes and also vibrational frequencies and moments of inertia for the reactants and the transition states. We have found that the B3PW91 DFT method together with a 6-311++G(2d,p) basis set gave the best agreement with experimental vibrational frequencies, chemical activation rate constants and isotope effects for 1,2-HF elimination from CF_3CH_3/CF_3CD_3.[26] The B3PW91/6-311++G(2d,p) computational methodology was adopted for $CF_2ClCF_2CH_3$ and $CF_2ClCF_2CD_3$. The vibrational frequencies, moments of inertia and the threshold energies were used to calculate unimolecular rate constants, branching ratios and isotope effects using the RRKM theory.[2] The RRKM model, the experimental and computed kinetic data are in Table 2 for $CF_2ClCF_2CH_3$. In Table 4 the RRKM rate constants, branching ratios, and kinetic isotope effects are compared to the experimental values for decomposition of chemically activated $CF_2ClCF_2CH_3$ and $CF_2ClCF_2CD_3$, including 1,2-FCl rearrangement and 2,3-HF elimination.

The average energy, $\langle E \rangle$, for the chemically activated $CF_2ClCF_2CH_3/CF_2ClCF_2CD_3$ was estimated from the sum of the computed C2−C3 bond dissociation energy and the computed thermal energy for the $CF_2ClCF_2CH_3/CF_2ClCF_2CD_3$ at 298 K. The B3PW91/6-311++G(2d,p) methodology was also used for these calculations. The $\langle E \rangle$ was 98.5 and 100. kcal/mol for $CF_2ClCF_2CH_3$ and for $CF_2ClCF_2CD_3$ respectively. An $\langle E \rangle$ near 100 kcal/mol has been found for $CF_3CH_2CF_3$, $CF_3CH_2CH_3$, and $CF_3CF_2CH_3$ chemically activated by combination of methyl or trifluoromethyl radicals with haloethyl radicals.[20,25]

The transition states and threshold energies for the 1,2-FCl rearrangement and 2,3-HF elimination for $CF_2ClCF_2CH_3$ are markedly similar. The 1,2-FCl threshold energies is only 1.2 kcal/mol lower than the E_o(HF) and the thermal preexponential factors, per unit reaction path, are nearly identical; see Table 2. Thus, the activation entropy, $\Delta S^\dagger$, would be similar on a unit reaction path basis; see Table 2. The only significant difference is a reaction path degeneracy of 4 for HF loss and $^2/_3$ for the rearrangement. A reaction path degeneracy of $^2/_3$ for rearrangement arises because we are using a torsional model for the RRKM calculations and only 2 of the 3 staggered conformers have the Cl on carbon one and the F on carbon two in an anti-configuration. A computed branching ratio of 4.0, favoring HF elimination, is largely a consequence of the larger reaction path degeneracy for HF elimination.

Table 3 has the RRKM model, the computed and experimental data for $CF_3CFClCH_3$ and $CF_3CFClCD_3$. The computed HCl/HF branching ratio is 20, supporting our assumption (see above) that all of the $CF_3CFClCH_3$ reacts by HCl loss; i.e., reaction 6b can be neglected in the derivation of eqs 11 and 12. The computed threshold energy, E_o(2,3-HCl) = 55.4 kcal/mol, for $CF_3CFClCH_3$ seems reasonable in comparison to the 54 kcal/mol estimated for CF_2ClCH_3.[12] Since the computed unimolecular rate constant for HCl elimination from $CF_3CFClCH_3$ is about 60 times larger than the rate constant for FCl rearrangement in $CF_2ClCF_2CH_3$ most of the $CF_3CFClCH_3$ would be expected to lose HCl, in accord with the experimental findings.

The computed rate constants in Table 4 are a factor of 4−10 too large for the dehydrohalogenation reactions and the 1,2-FCl computed rate constants are 16−18 times too large. Agreements with the experimental branching ratios are better, the computed ratio is a factor of 3.38 too large for both $CF_2ClCF_2CH_3$ and for $CF_2ClCF_2CD_3$. The absolute rate constants and the branching ratio depend strongly on the threshold energy barrier and for HF elimination from CF_3CH_3 we have found[26] that these DFT methods often underestimate the E_o's for HX elimination; thus the theoretical rate constants are too large. For example, using the B3PW91 DFT method with two different, commonly used basis sets, 6-31G(d′,p′) and aug-cc-pVDZ, gave threshold energies for CF_3CH_3 differing by 4.7 kcal/mol and the G2 value was 8.1 kcal/mol higher than the aug-cc-pVDZ result. At an average energy of 100 kcal/mol and using the same vibrational frequenices, an increase from 64 to 69 kcal/mol in the threshold energy lowers the RRKM rate constant by a factor of 8.2. An increase of 8 kcal/mol in E_o for G2 versus the DFT B3PW91/aug-cc-pVDZ lowers the rate constant by a factor of 24.2. More refined treatments for calculation of the threshold energies could easily give smaller rate constants that would improve the agreement, but until the 1,2-FCl rearrangement mechanism is confirmed, the additional effort is not warranted. The computed and experimental isotope effects show much better agreement, all are within the estimated experimental error. Because the kinetic isotope effect is mainly sensitive to the difference in the E_o(HX) versus E_o(DX) and this is determined by the zero point vibrational frequencies, the absolute threshold energies can be in serious error but the computed and experimental kinetic isotope effect can agree if the vibrational frequencies are accurate. For absolute rate constants and the kinetic isotope effects the experimental uncertainty is typically 20−50% because data from two separate analyses are compared.

Uncertainty is less in the branching ratio, typically 10−20%, because product yield ratios are measured in the same analysis. The general agreement for all the experimental data supports our proposed two-step mechanism for the 1,3-HCl elimination from chemically activated $CF_2ClCF_2CH_3$ and $CF_2ClCF_2CD_3$.

The proposed mechanism for 1,2-FCl migration is a "double-bridged" rearrangement transition state structure. Chloronium and bromonium ions are well-known examples of 3-centered bridged ions involving chlorine or bromine migration in solution. 1,2-Halogen migration (halogen = Cl, Br or I) in haloethyl radicals has been of considerable interest[27] with the primary focus on the relative stability of the symmetric versus the asymmetric bridged structure. Rearrangement of radicals via a 3-centered fluorine bridged transition state structure is much less common than migration of other halogens but it has been reported[28,29] for CF_2CH_2F radicals. Shaler and Morton[30] proposed a three-membered cyclic transition state for fluorine migration in ionized $(CH_3)_2CFCH_2C_6H_5$ and presented SCF computations on $C_4H_8F^+$ ions supporting 1,2-fluorine bridging. Fluorine migration has been implicated in the rearrangement of fluorocarbenes by Haseldine and co-workers[31] following photolysis of fluoro-substituted diazoalkanes or diazirines and by others[32,33] during decomposition of energized haloalkanes that formed fluorocarbenes. A 3-centered fluorine bridge has also been suggested during the IRMPD induced decomposition of tetrafluorocyclopropene[34] that produced tetrafluoropropyne, probably via a biradical process. These 1,2-halogen migrations all involve open shelled systems. The present work appears to be the first report suggesting a similar rearrangement process involving a double-bridge of two halogens in a closed shell molecule.

4. Conclusions

The experimental and computational results suggest that chemically activated $CF_2ClCF_2CH_3$ and $CF_2ClCF_2CD_3$ react via elimination of HF (DF) and also by a newly discovered 1,2-FCl rearrangement. Table 4 is a summary of the experimental and calculated rate constants. In general, there is acceptable agreement. Although the computed rate constants were always too large, probably because the threshold energy barriers were too low, the agreement between the experimental and computed rate constants and the FCl/HF branching ratio was satisfactory. Agreement between the computed and experimental isotope effects were within the experimental uncertainty. The close accord between the experimental and computed isotope effects for the 1,2-FCl rearrangement and for the elimination reactions (2,3-HF/DF and 2,3-HCl/DCl) strongly supports our proposed mechanism. We believe that this is the first evidence for a 1,2-FCl rearrangement and we are currently exploring similar systems to determine whether this is common process.

Acknowledgment. Support from the National Science Foundation, CHE-9904125, is gratefully acknowledged, as is time from the North Carolina Supercomputing Center.

References and Notes

(1) Maccoll, A. *Chem. Rev.* **1969**, *69*, 33.
(2) Holbrook, K. A.; Pilling, M. J.; Robertson, S. H. *Unimolecular Reactions*, 2nd ed.; Wiley: New York, 1996.
(3) Miyoshi, A.; Yamauchi, N.; Kosaka, K.; Koshi, M.; Matsui, H. *J. Phys. Chem. A* **1999**, *103*, 46.
(4) Kim, K. C.; Setser, D. W. *J. Phys. Chem.* **l974**, *78*, 2166.
(5) Kim, K. C.; Setser, D. W.; Holmes, B. E. *J. Phys. Chem.* **1973**, *77*, 725.
(6) Rakestraw, D. J.; Holmes, B. E. *J. Phys. Chem.* **1991**, *95*, 3968.
(7) Millward, G. C.; Tschuikow-Roux, E. *Int. J. Chem. Kinet.* **1972**, *4*, 559.
(8) Shapiro, J. S.; Swinbourne, E. S. *Can. J. Chem.* **1968**, *46*, 1341 and 1351.
(9) Holmes, J. L.; McGillivary, D. L.; Yuan, D. *Can. J. Chem.* **1979**, *57*, 2621.
(10) Failes, R. L.; Mollah, Y. M. A.; Shapiro, J. S. *Int. J. Chem. Kinet.* **1981**, *13*, 7.
(11) Failes, R. L.; Mollah, Y. M. A.; Shapiro, J. S. *Int. J. Chem. Kinet.* **1979**, *11*, 1271.
(12) McDoniel, J. B.; Holmes, B. E. *J. Phys. Chem.* **1996**, *100*, 3044.
(13) (a) Dees, K.; Setser, D. W. *J. Chem. Phys.* **1968**, *49*, 1193. (b) Clark, W. G.; Setser, D. W.; Dees, K. *J. Am. Chem. Soc.* **1971**, *93*, 5328.
(14) Lin, J. J.; Wu, S. M.; Hwang, D. W.; Lee, Y. T.; Yang, X. *J. Chem. Phys.* **1998**, *109*, 10838.
(15) Farmanara, P.; Stert, V.; Radloff, W. *Chem. Phys. Lett.* **1998**, *288*, 518.
(16) Lee, Y. R.; Wang, L. D.; Lee, Y. T.; Lin, S. M. *J. Chem. Phys.* **2000**, *113*, 5331.
(17) Lee, Y. R.; Wang, L. D.; Lee, Y. T.; Lin, S. M. *J. Chem. Phys.* **2000**, *113*, 6107.
(18) Melchior, A.; Bar, I.; Rosenwaks, S. *J. Chem. Phys.* **1997**, *107*, 8476.
(19) Holmes, B. E.; Paisley, S. D.; Rakestraw, D. J.; King, E. E. *Int. J. Chem. Kinet.* **1986**, *18*, 639.
(20) McDoniel, J. B.; Holmes, B. E. *J. Phys. Chem. A* **1997**, *101*, 1334.
(21) Jones, Y.; Holmes, B. E.; Duke, D. W.; Tipton, D. L. *J. Phys. Chem.* **1990**, *94*, 4957.
(22) Chang, H. W.; Setser, D. W. *J. Am. Chem.* Soc. **1969**, *91*, 7648.
(23) Kim, K. C.; Setser, D. W.; Holmes, B. E. *J. Phys. Chem.* **1973**, *77*, 725.
(24) Heard, G. L.; Holmes, B. E. *J. Phys. Chem. A* **2001**, *105*, 1622.
(25) Ferguson, H. A.; Ferguson, J. D.; Holmes, B. E. *J. Phys. Chem. A* **1998**, *102*, 5393.
(26) Martell, J.; Holmes, B. E. Submitted to *J. Phys. Chem.*
(27) Ihee, H. Seqail, A. H.; Goddard, W. A., III. *J. Phys. Chem. A* **1999**, *103*, 6638, and references therein.
(28) Kohida, R.; Kotaka, M.; Sato, S.; Ishida, R.; Yamamoto, K.; Yamazaki, T.; Kitazume, T *Bull. Chem. Soc. Jpn.* **1987**, *60*, 3131.
(29) Kotaka, M.; Sato, S. *J. Chem. Soc., Chem. Commun.* **1986**, 1783.
(30) Shaler, T. A.; Morton, T. H. *J. Am. Chem. Soc.* **1994**, *116*, 9222 and references therein.
(31) Haszeldine, R. N.; Parkinson, C.; Robinson, P. J.; Williams, W. J. *J. Chem. Soc., Perkin Trans. 2* **1979**, *954* and reference therein.
(32) Holmes, B. E.; Rakestraw, D. J. *J. Phys. Chem.* **1992**, *96*, 2210.
(33) Millward, G. C.; Tschuikow-Roux, E. *Int. J. Chem. Kinet.* **1972**, *4*, 559.
(34) Friedrich, H. B.; Burton, D. J.; Tardy, D. C. *J. Phys. Chem.* **1987**, *91*, 6334.